A New Discontinuous Galerkin Method for Hamilton-Jacobi Equations

Jue Yan[*] and Stanley Osher[†]

February 23, 2010

Abstract

In this paper we propose a new local discontinuous Galerkin method to directly solve Hamilton-Jacobi equations. The scheme is a natural extension of the monotone scheme. For the linear case, the method is equivalent to the discontinuous Galerkin method for conservation laws. Thus, stability and error analysis are obtained under the framework of conservation laws. For both convex and nonconvex Hamiltonian, optimal $(k+1)$-th order of accuracy for smooth solutions are obtained with piecewise k-th order polynomial approximations. The scheme is numerically tested on a variety of one and two dimensional problems. The method works well to capture sharp corners (discontinuous derivatives) and converges to the viscosity solution.

AMS subject classification: 35Q53

Key Words: Discontinuous Galerkin method, Hamilton-Jacobi equation.

Contents

1   Introduction

In this paper we develop a new discontinuous Galerkin (DG) finite element method to directly solve Hamilton-Jacobi (H-J) equations,

$$\Phi_t + H(\Phi_x, \Phi_y) = 0, \ \ (x,y) \in \Omega \tag{1.1}$$

augmented with suitable initial data $\Phi(x,y,0) = \Phi_0(x,y)$, and periodic boundary conditions. Hamilton-Jacobi equations arise in many applications areas, from optimal control theory and geometrical optics, to level set methods. Examples include crystal growth, ray tracing, etching, robotic motion planning, and computer vision.

Solutions to H-J equations are typically continuous but may develop singularities in the derivatives even if the initial condition is smooth. An appropriate definition of generalized solution must therefore be used, namely the viscosity solution, for which existence and uniqueness hold under suitable assumptions (see details in [11] by Crandall and Lions).

Finite difference type numerical methods for solving H-J equations have been well developed in the last two decades. In [12] Crandall and Lions first introduced a monotone numerical scheme to approximate H-J equations (1.1) and proved convergence to the viscosity solution. Later, a second order finite difference ENO scheme was developed by Osher and Sethian in [18], a general framework for higher-order ENO scheme was given by Shu and Osher in [19], and extension to a higher-order WENO scheme was proposed by Jiang and Peng in [15]. However, on an unstructured mesh the finite difference WENO scheme [24] is complicated to implement. Also for level set applications to two-phase flow, the interface is hard to track accurately with WENO scheme [13], which in the literature is called the "mass loss" problem. All these trigger the necessity to design other good algorithms to solve H-J equations.

The discontinuous Galerkin method is a finite element method using a completely discontinuous piecewise polynomial space for the numerical solution and the test functions. Major development of discontinuous Galerkin methods was carried out by Cockburn, Shu and their collaborators in a series of papers [7, 6, 5, 3, 9] for nonlinear hyperbolic conservation laws. While it was being actively developed, the DG method found rapid applications in many areas, see [4, 10]. Discontinuous Galerkin methods become attractive and popular due to the following nice features: 1) it is easy to apply high order approximations, thus allowing for efficient p adaptivity; 2) it is flexible on complicated geometries, thus allowing for efficient h adaptivity; 3) it is extremely local in data communications, thus allowing for efficient parallel implementations.

For solving H-J equations with discontinuous Galerkin method, however, there are conceptual difficulties. This is because the H-J equations cannot be written in a "conservation form", which is suitable for integration by parts, and is a crucial property for discontinuous Galerkin methods. On the other hand, it is well known that H-J equations are closely related to conservation laws. In the 1-D case we can claim they are equivalent. Based on this observation and the success of discontinuous Galerkin methods to conservation laws, Hu and Shu [14] developed a DG method for H-J equations in 1999. Recently in [2] Cheng and Shu proposed a new DG method directly solving H-J equations. Our goal is also to design a direct DG method for solving H-J equations. The DG method we use is essentially a local discontinuous Galerkin (LDG) method.

Local discontinuous Galerkin methods are designed to solve partial differential equations with higher order spatial derivatives. The idea is to introduce new variables to approximate the solution derivatives and rewrite the equation as a first order system, then apply the discontinuous Galerkin method for the system. The first LDG method was developed by Cockburn and Shu in [8] for the convection diffusion equation involving second order spatial derivatives. Their work was motivated by the successful numerical experiments of Bassi and Rebay [1] for the compressible Navier-Stokes equations. Later, Yan and Shu [23] developed a LDG method for the general KdV type equation involving third order spatial derivatives. Recently LDG methods have been rapidly developed for a large number of nonlinear problems, e.g. [16, 17, 22].

The procedure of applying LDG method to solve H-J equations is the following. First, we introduce 4 new variables p_1, p_2 and q_1, q_2 to respectively approximate Φ_x and Φ_y,

$$\begin{cases} p_1 - \Phi_x = 0 \\ p_2 - \Phi_x = 0 \end{cases} \quad \begin{cases} q_1 - \Phi_y = 0 \\ q_2 - \Phi_y = 0. \end{cases}$$

This is carried out by solving the standard upwind discontinuous Galerkin method, namely p_1 and p_2 are auxiliary variables used to approximate Φ_x with numerical flux chosen from the right (Φ_x^+) and the left (Φ_x^-) respectively, and q_1 and q_2 are used to approximate Φ_y^+ and Φ_y^- correspondingly. We see p_1 is identical to p_2 when the solution is smooth, but at the same time p_1 and p_2 can fully capture the characteristic of Φ_x when the solution have corners. Similarly, this mechanism guarantees q_1 and q_2 can capture complete information of Φ_y. Then we plug them into a monotone consistent numerical Hamiltonian $\hat{H}(p_1, p_2, q_1, q_2)$ and solve the H-J equation in the weak sense, namely multiply the equation by a test function and integrate over the element. Note here we use the numerical Hamiltonian $\hat{H}$ in the scheme formulation. With piecewise constant approximation, our scheme degenerates to the standard monotone scheme, that guarantees its convergence to the viscosity solution. In some sense, we can claim our scheme is a natural extension of the monotone scheme whithin DG framework.

For the linear constant coefficient case, the method is equivalent to the discontinuous Galerkin method for conservation laws. Thus, stability and error analysis are carried out in the same way as for conservation laws. For

the linear variable coefficient problem, our scheme is not exactly the same as the standard discontinuous Galerkin method, but the LDG scheme captures the characteristics correctly and numerically we obtain optimal order of accuracy with smooth variable coefficients. We test the LDG methods on a variety of one and two dimensional Hamilton-Jacobi equations. For both convex and nonconvex Hamiltonian, optimal $(k+1)$-th order of accuracy for smooth solutions are obtained with piecewise kth degree polynomial approximations. The method works well to capture sharp corners (discontinuous derivatives) and the LDG solution converges to the viscosity solution.

In this paper we use capital letters Φ etc. to denote the exact solutions to the H-J equations and lower case letters ϕ to denote the discontinuous Galerkin numerical solutions. This paper is organized as follows: In §2, we introduce the formulation of local discontinuous Galerkin method for the one-dimensional H-J equations. The generalization of LDG methods to two-dimensional H-J equations is discussed in §3. In §4, we present a series of numerical results to validate the LDG methods. Conclusions and remarks are given in §5.

2 The LDG scheme formulation and theoretical results for the one-dimensional case

In this section we define our LDG method for solving Hamilton-Jacobi equation(1.1) in one-dimensional setting,

$$\Phi_t + H(\Phi_x) = 0, \quad x \in \Omega. \tag{2.2}$$

First let's introduce some notations. The computational mesh is given by $\Omega = \{I_j = (x_{j-\frac{1}{2}}, x_{j+\frac{1}{2}}), \ j = 1, ..., N\}$. We denote $x_j = \frac{1}{2}\left(x_{j-\frac{1}{2}} + x_{j+\frac{1}{2}}\right)$ as the center of the cell I_j and $\Delta x_j = x_{j+\frac{1}{2}} - x_{j-\frac{1}{2}}$ as the size of each cell. We denote $\Delta x = \max_j \Delta x_j$. The numerical solution space $\mathcal{V}_{\Delta x}$ is defined as the piecewise polynomial space where there is no continuity requirement at the cell interface $x_{j\pm 1/2}$.

$$\mathcal{V}_{\Delta x} = \left\{ v \in L^2(\Omega) : \ v|_{I_j} \in P^k(I_j), \ j = 1, ..., N \right\}, \tag{2.3}$$

where $P^k(I_j)$ denotes the polynomial space on I_j with degree at most k. The local discontinuous Galerkin method is defined as the following: We seek a numerical solution $\phi \in \mathcal{V}_{\Delta x}$ such that for all test function $u \in \mathcal{V}_{\Delta x}$ we have,

$$\int_{I_j} \phi_t u \, dx + \int_{I_j} \widehat{H}(p_1, p_2) u \, dx = 0 \quad \forall j = 1, \cdots, N \tag{2.4}$$

where p_1 and p_2 are two new variables we introduce to approximate Φ_x, and $\widehat{H}(p_1, p_2)$ is the monotone consistent numerical Hamiltonian we choose to approximate $H(\Phi_x)$.

Just as those defined in the LDG method[8], p_1 and p_2 are two auxiliary variables. Both p_1 and p_2 are introduced to approximate Φ_x. Here p_1 is to

4

approximate Φ_x with numerical flux chosen from the right (upwind right), like ϕ_x^+ in [15]. In a word, for any test function $v \in \mathcal{V}_{\Delta x}$, p_1 is obtained by solving the following right upwind DG scheme,

$$\int_{I_j} p_1 v dx + \int_{I_j} \phi v_x dx - \phi_{j+1/2}^+ v_{j+1/2}^- + \phi_{j-1/2}^+ v_{j-1/2}^+ = 0. \qquad (2.5)$$

Variable p_2 is introduced to approximate Φ_x with the numerical flux chosen from the left (upwind left). For any test function $w \in \mathcal{V}_{\Delta x}$, p_2 is obtained through the following left upwind DG scheme,

$$\int_{I_j} p_2 w dx + \int_{I_j} \phi w_x dx - \phi_{j+1/2}^- w_{j+1/2}^- + \phi_{j-1/2}^- w_{j-1/2}^+ = 0. \qquad (2.6)$$

Finally we replace $H(\Phi_x)$ in equation (2.2) by a monotone consistent numerical Hamiltonian $\widehat{H}(p_1, p_2)$, for monotone we mean $\widehat{H}(\downarrow, \uparrow)$ that is a none increasing function for the fist argument and a none decreasing function for the second argument. For consistency we mean $\widehat{H}(p, p) = H(p)$. At each time step, we first locally compute p_1 and p_2 from (2.5) and (2.6), then plug p_1 and p_2 into the numerical Hamiltonian $\widehat{H}(p_1, p_2)$, multiply it with any test function $u \in \mathcal{V}_{\Delta x}$, integrate over cell I_j and update ϕ to the next time level. This completes the definition of the LDG scheme. For time discretization, we use explicit third-order TVD Runge-Kutta method as in [20].

In this paper, we simply use the Lax-Friedrichs numerical Hamiltonian,

$$\widehat{H}(p_1, p_2) = H(\frac{p_1 + p_2}{2}) - \frac{1}{2}\alpha(p_1 - p_2)$$

with $\alpha = \max_{p \in D}|\frac{\partial H(p)}{\partial p}|$. With D taken as a local domain, namely D is evaluated locally as $D = [min(p_1, p_2), max(p_1, p_2)]|_{I_j}$ we call it a local Lax-Friedrichs scheme. With D taken as a global domain, namely D is evaluated over the whole computational domain and defined as $D = [min(p_1, p_2), max(p_1, p_2)]|_\Omega$ we call it the global Lax-Friecrichs scheme.

Now we turn to the question of the quality of the numerical solution defined by the LDG method. If the Hamiltonian $H(\Phi_x)$ is a linear function, equation (2.2) degenerates to a linear wave equation (2.7), for simplicity we assume $a > 0$ is a constant.

$$\Phi_t + a\Phi_x = 0 \qquad (2.7)$$

Now the numerical Hamiltonian $\hat{H}(p_1, p_2)$ degenerates to a simple upwind flux ap_2, and LDG scheme (2.4)-(2.6) is simplified as follows:

$$\begin{cases} \int_{I_j} \phi_t u dx + \int_{I_j} ap_2 u dx = 0 \\ \int_{I_j} p_2 w dx + \int_{I_j} \phi w_x dx - \phi_{j+1/2}^- w_{j+1/2}^- + \phi_{j-1/2}^- w_{j-1/2}^+ = 0. \end{cases} \qquad (2.8)$$

It's easy to see, with the same test function $u = w$, the LDG scheme (2.8) is nothing but a standard upwind DG scheme. So we have the following optimal error estimate for the linear problem (2.7).

5

Proposition 2.1 (error estimate) *Suppose the exact solution Φ of (2.7) is smooth and numerical solution ϕ is obtained with our scheme (2.8). Let $e(\cdot, t)$ be the approximation error $\Phi - \phi$. Then we have,*

$$\|e(\cdot, T)\|_{L^2(\Omega)} \leq C|\Phi_0|^{k+2}(\Delta x)^{k+1}, \tag{2.9}$$

where C depends on k, a and the final time T.

For variable coefficient linear Hamilton-Jacobi equation

$$\Phi_t + a(x)\Phi_x = 0 \tag{2.10}$$

the scheme (2.4) becomes,

$$\int_{I_j} \phi_t u dx + \int_{I_j} \left\{ \frac{p_1}{2}(a(x) - |a(x)|)u + \frac{p_2}{2}(a(x) + |a(x)|)u \right\} dx = 0 \tag{2.11}$$

Note that even the scheme (2.11) is not exactly the same as the standard DG method for (2.10), however the scheme catches the upwind directions correctly, always takes p_2 with $a(x) > 0$ and p_1 with $a(x) < 0$. Numerically we obtain optimal $(k+1)$th order of accuracy for p^k polynomial approximations with smooth variable coefficient $a(x)$.

3 The LDG scheme formulation for the two dimensional case

In this section, we generalize the LDG scheme discussed in the previous section to the two spatial dimensions. The algorithm in more spatial dimensions is similar. For 2D, the scalar HJ equation is,

$$\Phi_t + H(\Phi_x, \Phi_y) = 0, \quad (x, y) \in [0, 1] \times [0, 1], \tag{3.12}$$

with initial condition $\Phi(x, y, 0) = \Phi_0(x, y)$ and periodic boundary conditions. Notice that the assumption of a unit box geometry and periodic boundary conditions is for simplicity only and is not essential: the method can be easily designed for arbitrary domain and for non-periodic boundary conditions.

Let's denote a triangulation of the unit box by $T_{\Delta x} = \{K\}$, consisting of non-overlapping polyhedra covering completely the unit box. We assume the triangles K to be shape-regular. Here $\Delta x = diam\{K\}$ measures the diameter of the triangle K. We again denote the finite element space by

$$\mathcal{V}_{\Delta x} = \left\{ v \in L^2 : \ v|_K \in P^k(K), \ \forall K \in T_{\Delta x} \right\}. \tag{3.13}$$

where $P^k(K)$ is the set of all polynomials of degree at most k on cell K. We propose a discontinuous Galerkin method for (3.12) as follows: we seek $\phi \in \mathcal{V}_{\Delta x}$ such that for all test function $u \in \mathcal{V}_{\Delta x}$ and all cells $K \in T_{\Delta x}$ we have,

$$\int_K \phi_t u \, dx dy + \int_K \widehat{H}(p_1, p_2, q_1, q_2) u \, dx dy = 0 \tag{3.14}$$

Here again $\widehat{H}(p_1, p_2, q_1, q_2)$ is a monotone consistent numerical Hamiltonian we choose to approximate $H(\Phi_x, \Phi_y)$. Four new auxiliary variables p_1, p_2 and q_1, q_2 are introduced to approximate Φ_x and Φ_y respectively.

Variables p_1 and p_2 are both used to approximate Φ_x. Similar to the 1D case, we obtain p_1 and p_2 by solving two simple upwind DG schemes. We seek $p_1 \in \mathcal{V}_{\Delta_x}$ and $p_2 \in \mathcal{V}_{\Delta_x}$ such that for any test functions $v_1 \in \mathcal{V}_{\Delta_x}$ and $v_2 \in \mathcal{V}_{\Delta_x}$ we have

$$\begin{cases} \int_K p_1 v_1 \, dxdy + \int_K \phi(v_1)_x \, dxdy - \int_{\partial K} \phi^+ n_x v_1^{int_K} ds = 0 \\ \int_K p_2 v_2 \, dxdy + \int_K \phi(v_2)_x \, dxdy - \int_{\partial K} \phi^- n_x v_2^{int_K} ds = 0 \end{cases} \quad (3.15)$$

with

$$\phi^+ = \begin{cases} \phi^{ext_K}, & \text{if } n_x \geq 0 \\ \phi^{int_K}, & \text{else} \end{cases}$$

and

$$\phi^- = \begin{cases} \phi^{int_K}, & \text{if } n_x \geq 0 \\ \phi^{ext_K}, & \text{else} \end{cases}$$

where ∂K is the boundary of element K, $n = (n_x, n_y)$ is the outward unit normal for element K along the element boundary ∂K. Here we use ϕ^{int_K} to denote the value of ϕ on ∂K evaluated from inside the element K. Correspondingly we use ϕ^{ext_K} to denote the value of ϕ on ∂K evaluated from the outside element K (inside the neighboring element K' which shares the same edge with K).

The two new variables q_1 and q_2 are used to approximate Φ_y and obtained by solving the following two upwind DG schemes. We seek $q_1 \in \mathcal{V}_{\Delta_x}$ and $q_2 \in \mathcal{V}_{\Delta_x}$ such that for any test functions $w_1 \in \mathcal{V}_{\Delta_x}$ and $w_2 \in \mathcal{V}_{\Delta_x}$ we have

$$\begin{cases} \int_K q_1 w_1 \, dxdy + \int_K \phi(w_1)_y \, dxdy - \int_{\partial K} \phi^+ n_y w_1^{int_K} ds = 0 \\ \int_K q_2 w_2 \, dxdy + \int_K \phi(w_2)_y \, dxdy - \int_{\partial K} \phi^- n_y w_2^{int_K} ds = 0 \end{cases} \quad (3.16)$$

with

$$\phi^+ = \begin{cases} \phi^{ext_K}, & \text{if } n_y \geq 0 \\ \phi^{int_K}, & \text{else} \end{cases}$$

and

$$\phi^- = \begin{cases} \phi^{int_K}, & \text{if } n_y \geq 0 \\ \phi^{ext_K}, & \text{else} \end{cases}.$$

Finally, to complete the definition of LDG scheme, we choose a monotone consistent numerical Hamiltonian $\widehat{H}(p_1, p_2, q_1, q_2)$, for monotone we mean $\widehat{H}(\downarrow, \uparrow, \downarrow, \uparrow)$ and for consistency we mean $\widehat{H}(p, p, q, q) = H(p, q)$. Then plug p_1, p_2, computed from (3.15) and q_1, q_2 computed from (3.16), into the numerical Hamiltonian $\widehat{H}(p_1, p_2, q_1, q_2)$, multiply it with any test function $u \in \mathcal{V}_{\Delta_x}$ and integrate over the element K and update $\phi(x, y, t)$ to the next time level.

Here we simply use the Lax-Friedrichs type numerical Hamiltonian,

$$\widehat{H}(p_1, p_2, q_1, q_2) = H(\frac{p_1 + p_2}{2}, \frac{q_1 + q_2}{2}) - \frac{1}{2}\alpha(p_1 - p_2) - \frac{1}{2}\beta(q_1 - q_2)$$

with

$$\alpha = \max_{p \in D \, q \in E} |\frac{\partial H(p,q)}{\partial p}|.$$

With $D = [\min(p_1, p_2), \max(p_1, p_2)]|_{\mathbf{\Omega}}$ and $E = [\min(q_1, q_2), \max(q_1, q_2)]|_{\mathbf{\Omega}}$ we call it the global Lax-Friedrichs scheme. If D and E are rather local domain, in a word, $D = [\min(p_1, p_2), \max(p_1, p_2)]|_{\mathbf{K}}$ and $E = [min(q_1, q_2), max(q_1, q_2)]|_{\mathbf{K}}$ we call it the local local Lax-Friecrichs scheme. Note similar fashion is applied to coefficient β

$$\beta = \max_{p \in D \, q \in E} |\frac{\partial H(p,q)}{\partial q}|.$$

4   Numerical Examples

In this section we provide a series of numerical examples to illustrate the accuracy and capacity of the LDG method for solving H-J equations. For time discretization explicit third order Runge-Kutta method [21, 20] is used. We obtain optimal order of accuracy with piecewise p^k polynomial approximations and capture the entropy solution for both convex and nonconvex Hamiltonian.

Example 4.1: variable coefficient linear Hamiltonian

$$\phi_t + \sin(x)\phi_x = 0, \quad 0 \le x \le 2\pi, \tag{4.17}$$

with initial condition $\phi(x, 0) = \sin(x)$ and periodic boundary condition. The exact solution is given as

$$\phi(x, t) = \sin(2\tan^{-1}(e^{-t}\tan(\frac{x}{2}))).$$

As discussed in §2, for variable coefficient linear problem(4.17) our LDG method (2.11) is not exactly the same as the standard DG method. We use this example to demonstrate that the same optimal order of accuracy can be obtained as the standard DG method for variable coefficient conservation laws. We compute the solution up to $t = 1$ and check the L^1 and L^∞ errors with refined mesh, $(k+1)$th order of accuracy is obtained with p^k polynomial approximations. Results are listed in Table 4.1.

Example 4.2: linear Hamiltonian with kink solutions

$$\phi_t + \phi_x = 0, \quad -1 \le x < 1, \tag{4.18}$$

with initial $\phi(x, 0) = g(x - 0.5)$ and periodic boundary condition, here

$$g(x) = -(\frac{\sqrt{3}}{2} + \frac{9}{2} + \frac{2\pi}{3})(x+1) + \begin{cases} 2\cos(\frac{3\pi x^2}{2}) - \sqrt{3}, & -1 \le x < -\frac{1}{3}; \\ \frac{3}{2} + \cos(2\pi x), & -\frac{1}{3} \le x < 0; \\ \frac{15}{2} - 3\cos(2\pi x), & 0 \le x < \frac{1}{3}; \\ \frac{28+4\pi+\cos(3\pi x)}{3} + 6\pi x(x-1), & \frac{1}{3} \le x < 1. \end{cases}$$

We take the example from [15], and use it to test the ability of our scheme to catch the kinks after a long term run. We compute the LDG numerical

k		N=40	N=80		N=160		N=320	
		error	error	order	error	order	error	order
0	L^1	2.47e-01	1.28e-01	0.95	6.52e-02	0.97	3.29e-02	0.99
	L^∞	1.93e-01	9.80e-02	0.98	4.95e-02	0.98	2.48e-02	0.99
1	L^1	8.95e-03	2.28e-03	1.97	5.79e-04	1.98	1.46e-04	1.99
	L^∞	1.63e-02	4.44e-03	1.87	1.15e-03	1.95	2.92e-04	1.98
2	L^1	3.63e-04	4.52e-05	3.00	5.67e-06	2.99	7.12e-07	2.99
	L^∞	5.87e-04	9.10e-05	2.70	1.31e-05	2.80	1.85e-06	2.83
3	L^1	1.43e-05	9.14e-07	3.97	5.79e-08	3.98	3.66e-09	3.98
	L^∞	2.74e-05	1.86e-06	3.88	1.24e-07	3.90	7.95e-09	3.97

Table 4.1: 1D variable coefficient linear problem (4.17). L^1 and L^∞ errors at $t = 1.0$. p^k polynomial approximations with $k = 0, 1, 2, 3$.

solution with piecewise linear and quadratic approximations up to $t = 32(16$ periods), see Figure 4.1. We can observe better resolution with increased order of approximation. Compared to finite difference ENO/WENO schemes in [15] and [24], the DG method can sharply capture corners with discontinuous derivatives even after a long term run (16 periods when $t = 32$).

Example 4.3: nonlinear convex Hamiltonian(1D Burgers Equation)

$$\phi_t + \frac{(\phi_x + 1)^2}{2} = 0, \quad x \in [-1, 1] \tag{4.19}$$

with $\phi(x, 0) = -\cos(\pi x)$ and periodic boundary condition.

The solution is smooth till the discontinuous derivative develops at $t = \frac{1.0}{\pi^2}$. We compute the L^1 and L^∞ errors at $t = \frac{0.5}{\pi^2}$ and $t = \frac{3.5}{\pi^2}$, before and after the singularity develops, and list the errors and orders in Table 4.2 and Table 4.3. For $t = \frac{3.5}{\pi^2}$, the errors are computed away from the singularity with distance 0.15. Here we use the global Lax-Friedrichs scheme for the numerical Hamiltonian and roughly $(k + 1)$th order of accuracy is obtained with p^k polynomial approximations. In Figure 4.2, we show the LDG approximation at $t = \frac{3.5}{\pi^2}$ with p^1 and p^2 polynomials. The corner is clearly resolved for both piecewise linear and quadratic approximations.

Another example is the Burgers equation with none smooth initial condition

$$\phi(x, 0) = \begin{cases} \pi - x, & x < \pi; \\ x - \pi, & x \geq \pi. \end{cases}$$

It is designed in [2] to check the convergence of the numerical solution to the entropy solution. In Figure 4.3 we plot the LDG numerical solution with piecewise linear and quadratic approximations, clearly the LDG solution opens up and converges to the entropy solution.

Example 4.4: 1D nonconvex Hamiltonian

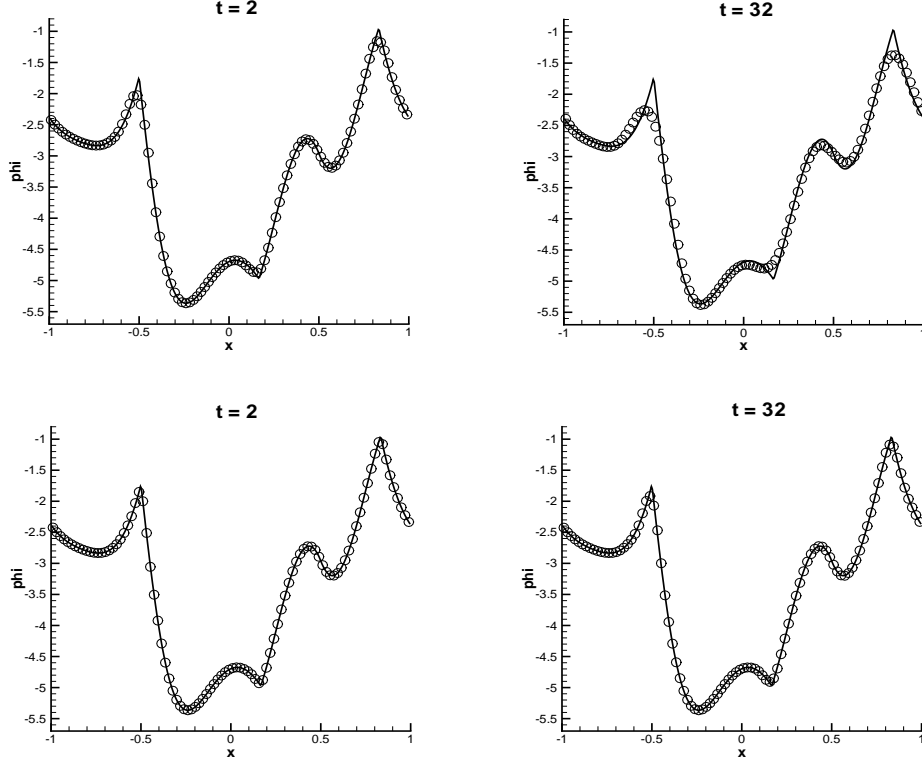$$\phi_t - \cos(\phi_x + 1) = 0, \quad x \in [-1, 1] \tag{4.20}$$

Figure 4.1: Solid line is the exact solution. Symbol circle is LDG approximation with mesh n=96. Top: linear approximation. Bottom: quadratic approximation.

k		N=20	N=40		N=80		N=160	
		error	error	order	error	order	error	order
0	L^1	1.35e-01	6.92e-02	0.96	3.51e-02	0.98	1.77e-02	0.99
	L^∞	1.73e-01	9.08e-02	0.92	4.67e-02	0.96	2.36e-02	0.98
1	L^1	6.56e-03	1.75e-03	1.91	4.31e-04	2.02	1.07e-04	2.00
	L^∞	1.34e-02	4.55e-03	1.56	1.12e-03	2.02	2.73e-04	2.03
2	L^1	2.26e-04	2.86e-05	2.98	3.57e-06	3.00	4.45e-07	3.00
	L^∞	1.25e-03	1.88e-04	2.73	2.41e-05	2.96	2.93e-06	3.05
3	L^1	9.57e-05	7.98e-06	3.58	6.21e-07	3.68	4.33e-08	3.84
	L^∞	2.35e-04	2.21e-05	3.41	1.75e-06	3.66	1.77e-07	3.30

Table 4.2: 1D Burgers equation. L^1 and L^∞ errors. p^k approximations with $k = 0, 1, 2, 3$ at $t = 0.5/\pi^2$.

k		N=20	N=40		N=80		N=160	
		error	error	order	error	order	error	order
0	L^1	1.80e-01	8.29e-02	1.11	3.98e-02	1.06	1.95e-02	1.02
	L^∞	2.63e-01	1.37e-01	0.94	6.95e-02	0.98	3.48e-02	1.00
1	L^1	7.89e-03	1.30e-03	2.60	2.25e-04	2.52	4.17e-05	2.43
	L^∞	3.93e-02	9.69e-03	2.02	2.32e-03	2.06	4.84e-04	2.26
2	L^1	7.15e-05	5.86e-06	3.60	6.78e-07	3.11	8.32e-08	3.02
	L^∞	6.59e-04	1.15e-05	5.83	1.31e-06	3.13	1.60e-07	3.03
3	L^1	4.54e-06	3.09e-07	3.87	1.76e-08	4.13	9.31e-10	4.24
	L^∞	1.07e-05	6.80e-07	3.97	4.20e-08	4.01	2.55e-09	4.04

Table 4.3: 1D Burgers equations. L^1 and L^∞ errors. p^k approximations with $k = 0, 1, 2, 3$ at $t = 3.5/\pi^2$.
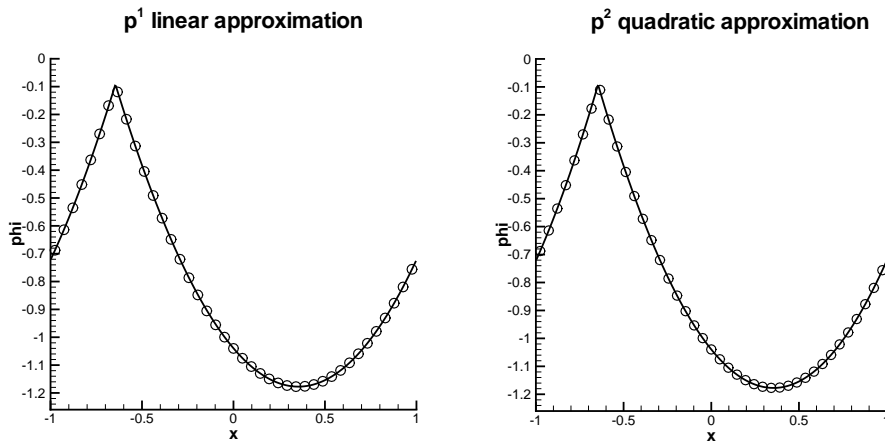

Figure 4.2: 1D Burgers equation at $t = \frac{3.5}{\pi^2}$ with mesh N=41. Solid line is the exact solution and symbol circle are the p^1 and p^2 polynomial approximations
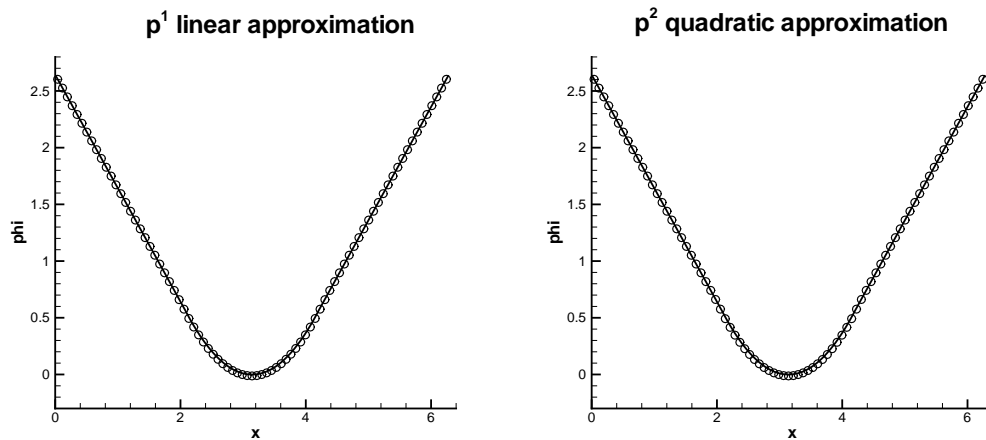
p¹ linear approximation   **p² quadratic approximation**

Figure 4.3: Solid line is the exact solution and symbol circle is p^1 and p^2 polynomial approximations at $t = 1$ with N=81.

k		N=20	N=40		N=80		N=160	
		error	error	order	error	order	error	order
0	L^1	1.03e-01	5.13e-02	1.00	2.56e-02	1.00	1.28e-02	1.00
	L^∞	1.44e-01	7.21e-02	1.00	3.61e-02	1.00	1.80e-02	1.00
1	L^1	6.01e-03	1.49e-03	2.01	3.69e-04	2.01	9.22e-05	1.99
	L^∞	2.11e-03	6.25e-04	1.75	1.44e-04	2.12	3.70e-05	1.96
2	L^1	2.90e-04	3.31e-05	3.13	4.19e-06	2.98	5.19e-07	3.01
	L^∞	2.22e-04	3.63e-05	2.61	5.66e-06	2.68	7.57e-07	2.90
3	L^1	1.22e-05	1.18e-06	3.36	7.59e-08	3.96	4.61e-09	4.04
	L^∞	8.39e-05	1.20e-05	2.80	1.35e-06	3.15	9.05e-08	3.91

Table 4.4: 1D nonconvex problem (4.20). L^1 and L^∞ errors. p^k polynomial approximations with $k = 0, 1, 2, 3$ at $t = 0.5/\pi^2$.

with $\phi(x, 0) = -\cos(\pi x)$ and periodic boundary condition.

Similar to the previous example, discontinuous derivative appears at $t = \frac{1.0}{\pi^2}$. We compute the L^1 and L^∞ errors and obtain $(k+1)$th order of accuracy for $t = \frac{0.5}{\pi^2}$ and $t = \frac{1.5}{\pi^2}$, before and after discontinuous derivatives developed, see Table 4.4 and Table 4.5. In Figure 4.4 we show the LDG approximations at $t = \frac{1.5}{\pi^2}$ and kinks are clearly resolved.

Example 4.5: 1D Riemann problem with nonconvex Hamiltonian

$$\phi_t - \frac{1}{4}(\phi_x^2 - 1)(\phi_x^2 - 4) = 0, \quad x \in [-1, 1] \tag{4.21}$$

with initial condition as $\phi(x, 0) = -2|x|$.

This is a benchmark problem to test a numerical scheme's capability to capture the entropy(viscosity) solution. The corresponding conservation law for ϕ_x have two shocks propagating to the left and right connected in between

k		N=20	N=40		N=80		N=160	
		error	error	order	error	order	error	order
0	L^1	5.02e-02	2.33e-02	1.10	1.17e-02	0.99	5.84e-03	1.00
	L^∞	1.72e-01	8.70e-02	0.98	4.36e-02	0.99	2.17e-02	1.00
1	L^1	3.18e-03	7.20e-04	2.14	1.75e-04	2.04	4.31e-05	2.02
	L^∞	1.42e-02	3.05e-03	2.22	7.53e-04	2.01	1.80e-04	2.02
2	L^1	7.26e-05	7.75e-06	3.22	9.47e-07	3.03	1.16e-07	3.01
	L^∞	7.84e-04	9.49e-05	3.04	1.25e-05	2.92	1.55e-06	3.01
3	L^1	5.50e-06	2.68e-07	4.35	1.70e-08	3.98	1.05e-09	4.01
	L^∞	4.57e-05	4.86e-06	3.23	3.26e-07	3.90	2.00e-08	4.02

Table 4.5: 1D noneconvex problem (4.20). L^1 and L^∞ errors. p^k polynomial approximations with $k = 0, 1, 2, 3$ at $t = 1.5/\pi^2$. Errors are computed in interval [-0.25,0] in which the solution is smooth.
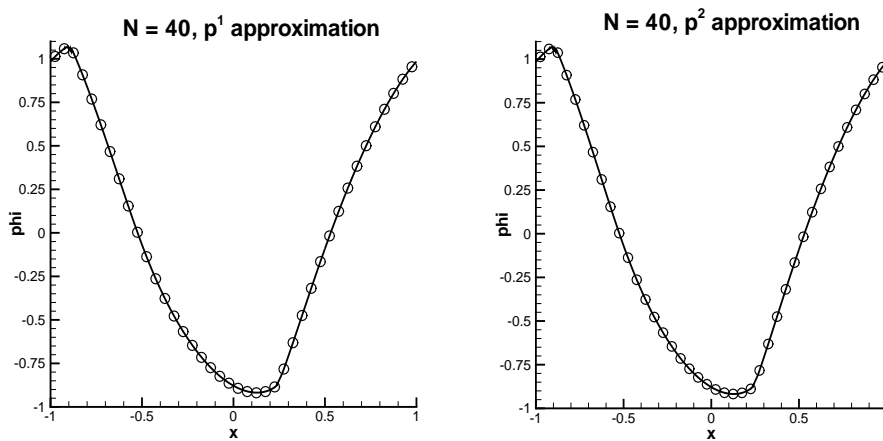

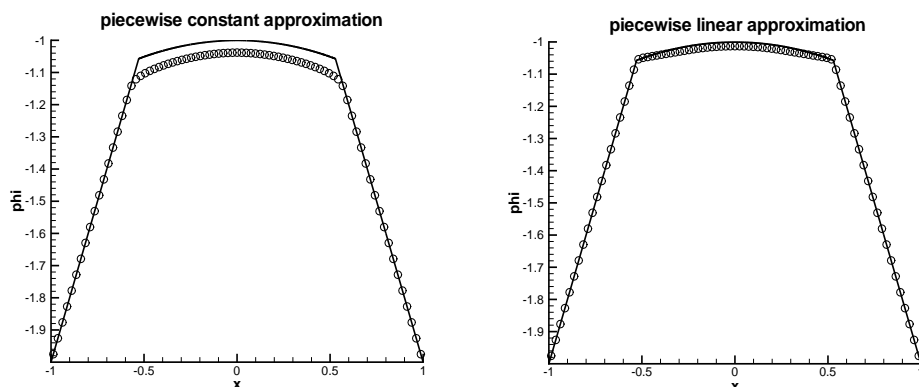Figure 4.4: 1D nonconvex Hamiltonian with piecewise linear and quadratic approximation at $t = 1.5/\pi^2$.

Figure 4.5: 1D Riemann problem with none convex Hamiltonian (4.21). mesh $N = 81$ at $t = 1$.

k		N=10	N=20		N=40		N=80	
		error	error	order	error	order	error	order
0	L^1	2.01e-01	1.03e-01	0.99	5.13e-02	1.00	2.56e-02	1.00
	L^∞	2.93e-01	1.44e-01	1.02	7.21e-02	1.00	3.61e-02	1.00
1	L^1	2.43e-02	6.01e-03	2.00	1.49e-03	2.01	3.69e-04	2.01
	L^∞	9.60e-03	2.88e-03	1.70	6.25e-04	1.75	1.44e-04	2.12
2	L^1	2.33e-03	2.90e-04	3.01	3.31e-05	3.13	4.19e-06	2.98
	L^∞	1.65e-03	2.22e-04	2.56	3.63e-05	2.61	5.66e-06	2.68

Table 4.6: 2D Burgers equations (4.22). L^1 and L^∞ errors at $t = \frac{0.5}{\pi^2}$. p^k polynomial approximation with $k = 0, 1, 2$.

with a rarefaction wave. With piecewise constant approximation our LDG scheme is monotone, and converges to the entropy solution. With piecewise linear or higher order approximations, limiter is needed for the convergence to the entropy solution. For this example and the 2D Riemann problem we use the TVB slope limiter as in [19]. Numerical results at $t = 1$ with 81 elements, using the local Lax-Friedrichs flux, is shown in Figure 4.5.

Example 4.6: 2D Burgers equation

$$\phi_t + \frac{(\phi_x + \phi_y + 1)^2}{2} = 0, \quad x \in \Omega = [-2, 2] X [-2, 2] \tag{4.22}$$

with initial condition $\phi(x, y, 0) = -\cos(\frac{\pi(x+y)}{2})$ and periodic boundary conditions.

We use local local Lax-Friedrichs numerical Hamiltonian in the computations. At $t = \frac{0.5}{\pi^2}$, the solution is still smooth. We compute the L^1 and L^∞ errors with $p^k(k = 0, 1, 2)$ polynomial approximations, and list the errors and order of accuracy in Table 4.6. At $t = \frac{1.5}{\pi^2}$ the discontinuous derivative has developed, the result of LDG solution is shown in Figure 4.6.
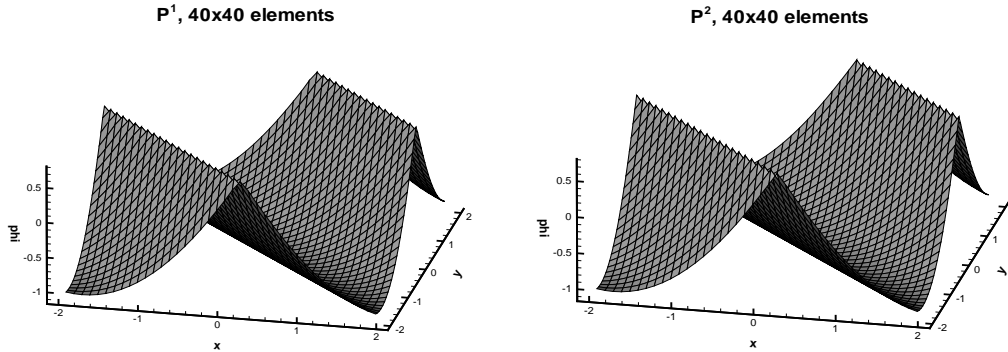
Figure 4.6: 2D Burgers equation (4.22) at $t = 1.5/\pi^2$ where corner has developed. p^1 polynomial approximation with mesh N=40X40.

k		N=10	N=20		N=40		N=80	
		error	error	order	error	order	error	order
0	L^1	1.35e-01	6.90e-02	0.97	3.47e-02	0.99	1.74e-02	1.00
	L^∞	6.07e-01	3.05e-01	0.99	1.51E-01	1.01	7.31e-02	1.05
1	L^1	5.34e-02	1.56e-02	1.78	4.03e-03	1.95	9.73e-04	2.05
	L^∞	1.02e-01	2.85e-02	1.84	7.80e-03	1.87	2.10e-03	1.90
2	L^1	7.83e-03	1.38e-03	2.50	2.12e-04	2.71	3.08e-05	2.78
	L^∞	4.48e-02	8.79e-03	2.35	1.52e-03	2.53	2.55e-04	2.58

Table 4.7: 2D problem with nonconvex Hamiltonian (4.23). L^1 and L^∞ errors at $t = \frac{0.5}{\pi^2}$. with $k = 0, 1, 2, 3$.

Example 4.7: 2D problem with nonconvex Hamiltonian

$$\phi_t - \cos(\phi_x + \phi_y + 1) = 0, \quad (x, y) \in \Omega = [-2, 2]X[-2, 2] \qquad (4.23)$$

with initial condition $\phi(x, y, 0) = -\cos(\frac{\pi(x+y)}{2})$ and periodic boundary conditions. Similar to the previous case, the solution develops discontinuous derivatives at $t = \frac{1.0}{\pi^2}$. We check the LDG errors and order of convergence at $t = \frac{0.5}{\pi^2}$, and we obtain $(k+1)$th order of accuracy, see Table 4.7. Figure 4.7 shows the LDG numerical solution approximation at $t = \frac{1.5}{\pi^2}$ where corners have developed.

Example 4.8: 2D Riemann problem

$$\phi_t + sin(\phi_x + \phi_y) = 0, \quad x \in \Omega = [-1, 1]X[-1, 1] \qquad (4.24)$$

with initial condition $\phi(x, y, 0) = \pi(|y| - |x|)$. With piecewise constant approximation LDG scheme degenerates to the monotone scheme, so it converges to the viscosity solution. With piecewise linear or higher order poly-
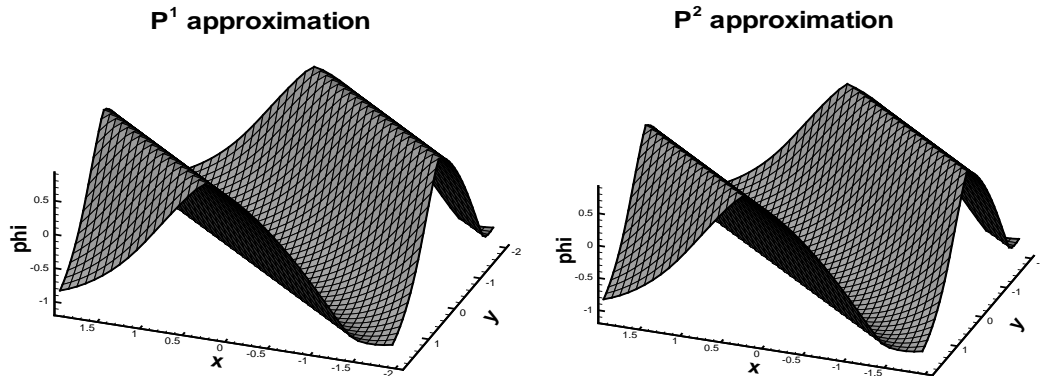
Figure 4.7: 2D equation with none convex Hamiltonian (4.23). $t = \frac{1.5}{\pi^2}$, p^1 and p^2 polynomial approximations with mesh N=40X40.
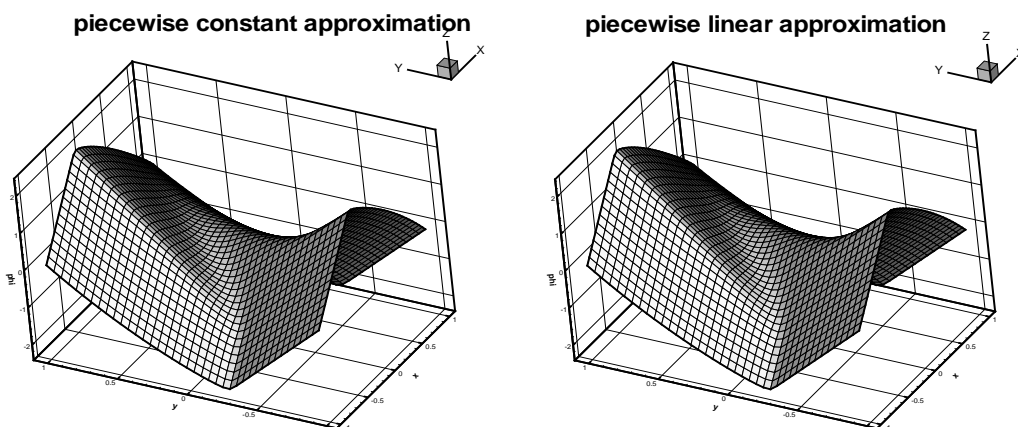

Figure 4.8: 2D Riemann problem (4.24) at $t = 1$, piecewise constant and linear polynomial approximation with mesh N=40X40.

nomial approximations, we need limiters in this example to have its convergence to the viscosity solution. LDG approximation with mesh $N = 40x40$ at $t = 1$ is listed in Figure 4.8.

5 Conclusions and Remarks

We propose a local discontinuous Galerkin method for directly solving Hamilton-Jacobi equations. For both convex and nonconvex Hamiltonian, optimal (k+1)-th order of accuracy for smooth solutions are obtained with piecewise k-th polynomial approximations. The method works well to capture sharp corners(discontinuous derivatives) and converges to the viscosity solution.

References

[1] F. Bassi and S. Rebay. A high-order accurate discontinuous finite element method for the numerical solution of the compressible Navier-Stokes equations. *J. Comput. Phys.*, 131(2):267–279, 1997.

[2] Y. Cheng and C.-W. Shu. A discontinuous Galerkin finite element method for directly solving the Hamilton-Jacobi equations. *J. Comput. Phys.*, 223(1):398–415, 2007.

[3] B. Cockburn, S. Hou, and C.-W. Shu. The Runge-Kutta local projection discontinuous Galerkin finite element method for conservation laws. IV. The multidimensional case. *Math. Comp.*, 54(190):545–581, 1990.

[4] B. Cockburn, G. E. Karniadakis, and C.-W. Shu. The development of discontinuous Galerkin methods. In *Discontinuous Galerkin methods (Newport, RI, 1999)*, volume 11 of *Lect. Notes Comput. Sci. Eng.*, pages 3–50. Springer, Berlin, 2000.

[5] B. Cockburn, S. Y. Lin, and C.-W. Shu. TVB Runge-Kutta local projection discontinuous Galerkin finite element method for conservation laws. III. One-dimensional systems. *J. Comput. Phys.*, 84(1):90–113, 1989.

[6] B. Cockburn and C.-W. Shu. TVB Runge-Kutta local projection discontinuous Galerkin finite element method for conservation laws. II. General framework. *Math. Comp.*, 52(186):411–435, 1989.

[7] B. Cockburn and C.-W. Shu. The Runge-Kutta local projection P^1-discontinuous-Galerkin finite element method for scalar conservation laws. *RAIRO Modél. Math. Anal. Numér.*, 25(3):337–361, 1991.

[8] B. Cockburn and C.-W. Shu. The local discontinuous Galerkin method for time-dependent convection-diffusion systems. *SIAM J. Numer. Anal.*, 35(6):2440–2463 (electronic), 1998.

[9] B. Cockburn and C.-W. Shu. The Runge-Kutta discontinuous Galerkin method for conservation laws. V. Multidimensional systems. *J. Comput. Phys.*, 141(2):199–224, 1998.

[10] B. Cockburn and C.-W. Shu. Runge-Kutta discontinuous Galerkin methods for convection-dominated problems. *J. Sci. Comput.*, 16(3):173–261, 2001.

[11] M. G. Crandall and P.-L. Lions. Viscosity solutions of Hamilton-Jacobi equations. *Trans. Amer. Math. Soc.*, 277(1):1–42, 1983.

[12] M. G. Crandall and P.-L. Lions. Two approximations of solutions of Hamilton-Jacobi equations. *Math. Comp.*, 43(167):1–19, 1984.

[13] D. Enright, R. Fedkiw, J. Ferziger, and I. Mitchell. A hybrid particle level set method for improved interface capturing. *J. Comput. Phys.*, 183(1):83–116, 2002.

[14] C. Hu and C.-W. Shu. A discontinuous Galerkin finite element method for Hamilton-Jacobi equations. *SIAM J. Sci. Comput.*, 21(2):666–690 (electronic), 1999.

[15] G.-S. Jiang and D. Peng. Weighted ENO schemes for Hamilton-Jacobi equations. *SIAM J. Sci. Comput.*, 21(6):2126–2143 (electronic), 2000.

[16] D. Levy, C.-W. Shu, and J. Yan. Local discontinuous Galerkin methods for nonlinear dispersive equations. *J. Comput. Phys.*, 196(2):751–772, 2004.

[17] H. Liu and J. Yan. A local discontinuous Galerkin method for the Korteweg-de Vries equation with boundary effect. *J. Comput. Phys.*, 215(1):197–218, 2006.

[18] S. Osher and J. A. Sethian. Fronts propagating with curvature-dependent speed: algorithms based on Hamilton-Jacobi formulations. *J. Comput. Phys.*, 79(1):12–49, 1988.

[19] S. Osher and C.-W. Shu. High-order essentially nonoscillatory schemes for Hamilton-Jacobi equations. *SIAM J. Numer. Anal.*, 28(4):907–922, 1991.

[20] C.-W. Shu and S. Osher. Efficient implementation of essentially nonoscillatory shock-capturing schemes. *J. Comput. Phys.*, 77(2):439–471, 1988.

[21] C.-W. Shu and S. Osher. Efficient implementation of essentially nonoscillatory shock-capturing schemes. II. *J. Comput. Phys.*, 83(1):32–78, 1989.

[22] Y. Xu and C.-W. Shu. Local discontinuous Galerkin methods for nonlinear Schrödinger equations. *J. Comput. Phys.*, 205(1):72–97, 2005.

[23] J. Yan and C.-W. Shu. A local discontinuous Galerkin method for KdV type equations. *SIAM J. Numer. Anal.*, 40(2):769–791 (electronic), 2002.

[24] Y.-T. Zhang and C.-W. Shu. High-order WENO schemes for Hamilton-Jacobi equations on triangular meshes. *SIAM J. Sci. Comput.*, 24(3):1005–1030 (electronic), 2002.